Inelastic neutron scattering studies of $TbNiAlH_{1.4}$ and $UNiAlH_{2.0}$ hydrides

2003 J. Phys.: Condens. Matter 15 2551

(http://iopscience.iop.org/0953-8984/15/17/310)

INSTITUTE OF PHYSICS PUBLISHING JOURNAL OF PHYSICS: CONDENSED MATTER

J. Phys.: Condens. Matter **15** (2003) 2551–2559 PII: S0953-8984(03)57070-9

Inelastic neutron scattering studies of $TbNiAlH_{1.4}$ and $UNiAlH_{2.0}$ hydrides

H N Bordallo[1,2,8], A I Kolesnikov[1], A V Kolomiets[3], W Kalceff[4], H Nakotte[5] and J Eckert[6,7]

[1] Intense Pulsed Neutron Source, Argonne National Laboratory, Argonne, IL 60439, USA
[2] Hahn-Meitner Institut, SF-1, Glienicker Straße, 100, D-14109, Berlin, Germany
[3] Department of Electronic Structures, Charles University, 12116 Prague 2, Czech Republic
[4] Department of Applied Physics, University of Technology Sydney, NSW 2007, Australia
[5] Physics Department, New Mexico State University, Las Cruces, NM 88003, USA
[6] Los Alamos Neutron Science Center, Los Alamos National Laboratory, Los Alamos, NM 87545, USA
[7] Materials Research Laboratory, University of California, Santa Barbara, CA 93106, USA

E-mail: bordallo@hmi.de

Received 3 December 2002
Published 22 April 2003
Online at stacks.iop.org/JPhysCM/15/2551

Abstract

The optical vibrations of hydrogen in $TbNiAlH_{1.4}$ and $UNiAlH_{2.0}$ were investigated by means of inelastic neutron scattering. The experimental data were analysed, including multiphonon neutron scattering contributions, calculated in an isotropic harmonic approximation. At least two fundamental H optical peaks were observed in $TbNiAlH_{1.4}$, and were assigned to the vibrational modes of hydrogen atoms occupying different interstitial sites in the metal sublattice. The high-energy part of the $UNiAlH_{2.0}$ spectra is characterized by strong anharmonicity, and a broad fundamental band. The latter can be accounted for by a large dispersion of phonon modes due to the strong H–H interactions, and/or different metal–hydrogen force constants, which may originate from different metal atoms surrounding the H atoms in the unit cell.

(Some figures in this article are in colour only in the electronic version)

1. Introduction

Isostructural RENiAl (RE = rare-earth atom) and UNiAl intermetallics have been the focus of scientific interest because of a variety of anomalous physical phenomena, particularly their magnetic properties, which are determined by the RKKY exchange interaction in the RENiAl ternaries [1, 2], and the 5f–5f and 5f–ligand hybridization effects in UNiAl [3, 4]. Different degrees of localization of the f states, and consequently the type of magnetic exchange, causes

[8] Address for correspondence: Hahn-Meitner-Institut Berlin–SF 1, D-14109 Berlin, Germany.

opposite effects in RE and U materials upon hydrogenation. Magnetic ordering is suppressed in the RENiAl series [5], but the Néel temperature of UNiAl increases by a factor of five upon hydrogen absorption [6, 7].

Detailed structural studies reveal that the crystal lattice also responds differently to hydrogenation of RENiAl and UNiAl. In both cases the parent compounds crystallize in the hexagonal ZrNiAl-type structure (space group $P\bar{6}2m$) [1, 4], but $TbNiAlD_x$ and $UNiAlH(D)_x$ have different structures depending on the degree of hydrogenation. For example, it has been shown that for a hydrogen (deuterium) content below $x = 0.67$ the symmetry of $TbNiAlD_x$ is hexagonal as in TbNiAl [8], but increased hydrogen absorption leads to an orthorhombic distortion of the unit cell (space group $Amm2$) [5, 7]. The structural changes observed in $UNiAlH_x$ are the opposite of those in $TbNiAlH_x$. While an orthorhombic distortion (space group $Pnma$) was reported for small x ($x \leqslant 0.58$), the hexagonal symmetry is recovered with higher hydrogen loading [9].

A fundamental question in the research on metal–hydrogen systems is the nature of the effective hydrogen single-particle potential in these systems. The energies of the hydrogen optical modes and their dispersion reflect the hydrogen potential, which depends on the chemical and topological environment around the hydrogen atom (i.e. crystal symmetry, interatomic separations, lattice distortion, and the type of the metal atoms in the host), and also the strength of the H–H interaction. This potential can be determined experimentally by analysing the excitation energy of the hydrogen optical modes and their dispersion in an inelastic neutron scattering (INS) experiment, which selectively probes the hydrogen motion because of its large neutron scattering cross-section [10].

We selected $TbNiAlH_{1.4}$ and $UNiAlH_{2.0}$ as model compounds that represent both 4f- and 5f-electron systems. The vibrational spectra of hydrogen atoms were measured using INS techniques. Peak assignments were carried out with the aid of multiphonon neutron scattering (MPNS) calculations in an isotropic harmonic approximation. The results are discussed in terms of the different sites occupied by the hydrogen atoms in these compounds. A brief comment to clarify contradictions [11–13] in the structure of $UNiAlD_{2.1}$ is also given.

2. Experimental details

Samples were prepared by arc melting of the parent components under an argon atmosphere. Melting was repeated several times in order to achieve high homogeneity of the samples. The higher evaporation rate of Tb in TbNiAl was compensated for by adding an extra $\sim$2 wt.% of this metal. X-ray diffraction analysis confirmed that the resulting compounds were single-phase TbNiAl and UNiAl polycrystals with the hexagonal ZrNiAl-type structure. The hydrides were then prepared by a two-step procedure: first, the intermetallic compounds were crushed and kept at 623 K under a vacuum of $\sim 10^{-6}$ Torr for 1 h; subsequently they were cooled to room temperature and exposed to a hydrogen atmosphere at pressures of 50 and 10 atm, respectively, for UNiAl and TbNiAl. The amount of absorbed hydrogen was determined by monitoring the decrease of pressure in a calibrated volume and the quality of the resulting compounds was checked by means of x-ray diffraction.

The INS spectra were collected at low temperatures ($T = 20$ K) using the Filter Difference Spectrometer at the Lujan Center of Los Alamos National Laboratory. Hydrogenated samples of $UNiAlH_{2.0}$ and $TbNiAlH_{1.4}$ were sealed under a helium atmosphere in annular cylindrical cans with a sample thickness of 1 mm. The spectra shown by solid lines with points in figures 1 and 2 were obtained by numerical deconvolution of the instrumental function [14] from the raw data after subtracting the sample container background measured under identical conditions.

In order to gain insight into the origin of the lineshapes of the high-energy part of the observed optical phonon bands, we have calculated the multiphonon contributions to the INS

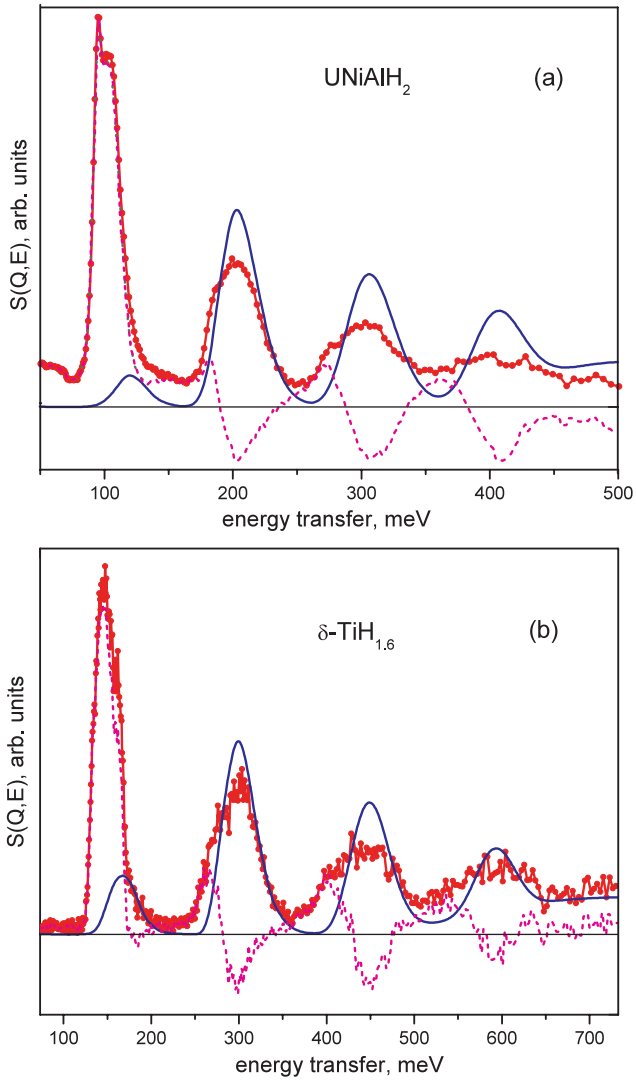

Figure 1. The INS spectrum for $UNiAlH_{2.0}$, (a), compared with that for δ-$TiH_{1.6}$ [19], (b). The experimental data are shown with points, while the solid curves show the calculated MPNS contributions, and the short dashed curves show their differences. In the range of the fundamental H optical band for $UNiAlH_{2.0}$, 75–130 meV, the dotted curve shows a fit of the difference curve with two Gaussian functions. A strong anharmonicity for the high-energy part of the spectrum is observed. The higher background observed in $UNiAlH_{2.0}$ is related to defects of the crystal structure.

spectra (MPNS) in an isotropic harmonic approximation. The results of this calculation also serve to help visualize the degree of anharmonicity evident in the hydride optical vibrations. Details of this procedure are provided in the appendix.

3. Results and discussion

Interpretation of the INS vibrational spectra in the first instance requires structural knowledge of the two compounds, particularly the location of the H atoms (number of sites; site symmetry;

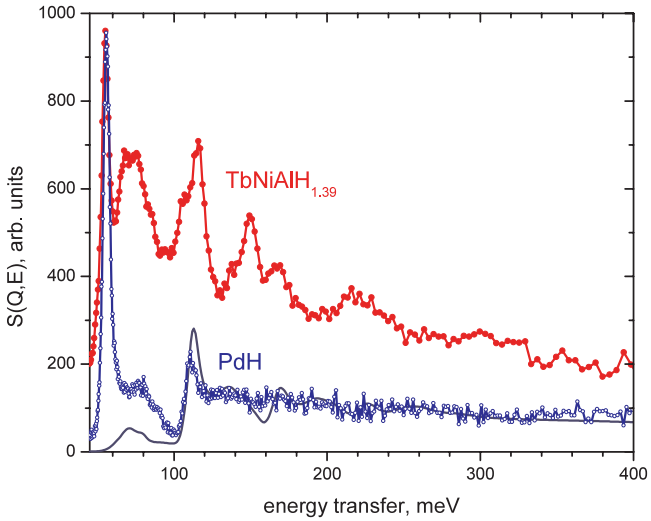

Figure 2. The INS spectrum for $TbNiAlH_{1.4}$ compared with the spectrum for PdH [23]. The curves with points show the experimental spectra; the solid curve shows the calculated MPNS contribution for PdH data.

types of nearest-neighbour metal atom). The results of previous structural work [15–17] on $TbNiAlD_x$, $UNiAlH_x$ and $UNiAlD_x$ show that for $x > 1$ the unit cell of $TbNiAlD_x$ contains at least two different partially occupied interstitial sites for D: a trigonal–bipyramidal Tb_3Ni_2-type site (site 4e) and a Tb_2NiAl tetrahedral site (4d). On the other hand, as many as five deuterium sites have been proposed for hexagonal $UNiAlD_x$ ($x \geqslant 0.7$) by various authors [11–13]. Because of the discrepancy between the different studies concerning the D locations, we have reanalysed the structure of $UNiAlD_{2.1}$, using a GSAS [18] refinement of neutron [11] and synchrotron x-ray diffraction data[9]. Figure 3 shows a portion of the observed and fitted neutron data ~0.5–3.7 Å which contains 355 reflections. Using the acentric primitive hexagonal space group $P\bar{6}2m$ with three formula units per unit cell, we obtain lattice parameters $a = 7.1892$ Å and $c = 3.9931$ Å, with $R_{wp} = 8.6\%$ and $R_p = 6.2\%$. Our refinements demonstrate that the atomic occupancies and fractional coordinates proposed by Raj *et al* [13] produce better fits than those reported in [7] and [11]. In this scheme, all Ni atoms occupy Ni–Al planes at $z = 0$, and all D atoms lie close to the U plane, rather than in the bipyramidal interstitial sites of the Al_3Ni_2 type.

Since the hydrogen atoms are apparently distributed over more than one inequivalent site with non-cubic local symmetry, as many as three $0 \rightarrow 1$ oscillator transitions per site could in principle occur, which may in turn lead to a rather complicated INS spectrum. An additional degree of complexity may be introduced by the fact that the nearest-neighbour H–H distance is rather small (~2.4 Å) which could, along with possible long-range H–H interaction, result in significant dispersion in H optical branches. The observed broadening and splittings of the fundamental hydrogen optical bands of these hydrides must therefore be discussed both in terms of multiple hydrogen site occupation and H–H interactions.

The INS spectrum of $UNiAlH_{2.0}$ at 20 K (figure 1(a)) shows peaks at approximately 100, 200, 300, and 400 meV. The MPNS contribution to the spectrum calculated in the harmonic

[9] Room temperature synchrotron XRD data were collected on beamline 12BM-B (BESSRC-CAT) at the Advanced Photon Source. Data were acquired for $10^\circ \leqslant 2\theta \leqslant 130^\circ$ using a 2θ step size of 0.001° and $\lambda = 0.103\,27$ Å.

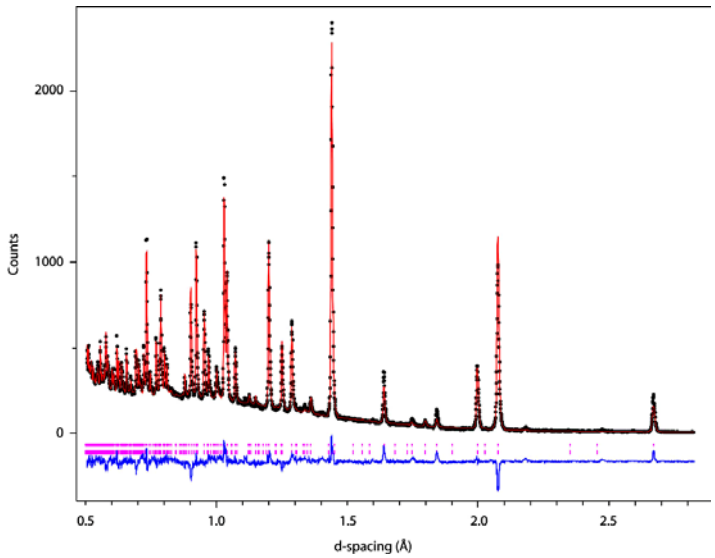

Figure 3. The room temperature neutron diffraction pattern obtained for $UNiAlD_{2.0}$. The experimental data are shown as points and the Rietveld fit as a solid curve. The bottom trace represents the difference between experimental and calculated intensities. In this figure we observe that the impurity peaks could not be successfully indexed.

isotropic approximation assuming that the fundamental H optical peak is in the range 75–130 meV is shown in the figure by the solid curve. A comparison of the calculated MPNS and experimental data clearly shows that the high-energy peaks of the experimental spectrum gradually decrease in intensity, broaden, and shift to lower energies. This indicates the presence of anharmonicity in the H potential in the crystal, i.e. it becomes shallower at higher energy compared with a purely harmonic form. After correction for the MPNS contribution, the fundamental H optic mode peak is well described by two Gaussian functions with positions at 93.7 meV (FWHM = 7 meV) and 103 meV (FWHM = 20 meV), and an intensity ratio of $I(E = 103)/I(E = 93.7) = 5.55$. The large deviation of this ratio from what would be expected for this type of site (i.e. 2.0) indicates that the shape of the fundamental H optical mode is strongly affected by the dispersion of the H optical phonon modes, the non-cubic local symmetry of the H site, and likely differences in metal–hydrogen force constants for different neighbouring metal atoms.

The $UNiAlH_{2.0}$ spectrum is compared with that of fcc δ-$TiH_{1.6}$ [19] in figure 1(b). For δ-$TiH_{1.6}$, the H atoms occupy tetrahedral interstitial positions in the metal sublattice. In this case, the fundamental hydrogen optical band has a complicated fine structure due to strong H–H interaction and it has been shown [19] that bound multiphonon states are formed at higher energies. These appear in the INS spectrum as hump-shaped features on the low-energy side of the normal multiphonon bands. The theoretical background for bound phonon states is given in [20–23], where it is shown that such bound multiphonon states can only occur in anharmonic crystals. Because of the apparent similarity of the INS spectra for $UNiAlH_{2.0}$ and δ-$TiH_{1.6}$, we propose that such bound multiphonon states may also occur in $UNiAlH_{2.0}$.

The INS spectrum for $TbNiAlH_{1.4}$ at 20 K is shown in figure 2. As mentioned in [17], considering the range of the fundamental H vibrations (up to 100 meV), we can identify two main vibrational bands at around 55 and 72 meV, where the latter is split into peaks at approximately 68 and 75 meV. Strong peaks (positions given are approximate) are also

observed at 116 meV (with a shoulder at 107 meV) and 150 meV (with a shoulder at 138 meV and sub-peak at 167 meV), and a broad peak at 220 meV.

We also compare the INS spectrum for $TbNiAlH_{1.4}$ with that of PdH [24] in figure 2, where the H atoms occupy octahedral interstitial positions in the Pd fcc lattice. The high-energy part (>100 meV) of the spectrum for polycrystalline PdH can reasonably be described by MPNS calculated in the harmonic isotropic approximation and multiple convolution of the fundamental H optical bands below 100 meV (see the solid curve in figure 2). Figure 2 demonstrates that the INS spectra of the two compounds show rather similar features: a sharp peak (at 55 meV) with an intense broad shoulder at about 75 meV, and a second sharp peak at approximately 112 meV. While PdH can be treated assuming single-site occupancy of the H atoms and with a fundamental H optical band assigned below 93 meV, the MPNS spectrum (solid curve 2; figure 4(a)), calculated for $TbNiAlH_{1.4}$ in the same manner, does not agree with the experimental data. This is evident from the fact that the peak at 113 meV is not reproduced when making the assumption that the fundamental optic phonon band in $TbNiAlH_{1.4}$ is also located below 93 meV. The agreement is not improved if the energy range for the fundamental band is extended to 130 meV (dashed curve 3 in figure 4(a)) as is evidenced by the fact that the peak at 148 meV is not reproduced.

The H atoms in $TbNiAlH_{1.4}$, however, occupy two inequivalent positions in the metal sublattice, and the peaks at 55 and 72 meV may therefore reasonably be assigned as the fundamentals from H atoms occupying the two different sites. We show the separate contributions (dashed and dotted curves in figure 4(b)) to the MPNS obtained by assuming that one-phonon parts for the two sites are confined to the bands at 55 and around 72 meV, respectively. The solid curve in figure 4(b) represents their sum and appears to fit the data reasonably well. This model thus reproduces the main features of the experimental data: the positions of the MPNS peaks are within acceptable limits, at about 116, 150, and 220 meV. The experimental intensity, however, appears to decrease faster with energy than the calculated curve. This discrepancy can again be attributed to the anharmonicity in the H-atom potentials, which results in shifts of the MPNS peaks. In the case of a small barrier height between the potential minima (and a shallow potential at higher energies), we expect the INS spectrum to show a gradual decrease in intensity of the higher-energy peaks as well as a shift to lower energies.

As far as the fundamental H optical peaks are concerned, we note that the low-energy one-phonon peak (at 55 meV) is very sharp, while the peak at higher energy (around 72 meV) is broad and split into two peaks. These observations suggest that the H atoms in sites corresponding to the peak at 55 meV are weakly interacting with each other, and are probably situated in an almost isotropic potential well. The width and splitting of the peak around 72 meV, on the other hand, may arise from dispersion of the corresponding H optical phonon branches resulting from strong H–H interactions, the non-cubic symmetry of the corresponding H potential, or perhaps a combination of these two effects. The anisotropy and anharmonicity of the potential would also explain the discrepancy between the experimental data and the MPNS spectrum calculated in the harmonic isotropic approximation.

4. Conclusions

We have interpreted the INS spectra of $UNiAlH_{2.0}$ and $TbNiAlH_{1.4}$ with the aid of MPNS calculations and find that the H modes in $UNiAlH_{2.0}$ originate from hydrogen atoms which occupy rather similar positions in the lattice and exhibit strong H–H interaction. The INS spectrum of $TbNiAlH_{1.4}$, on the other hand, can be explained in terms H occupation of at least two different sites in the metal sublattice and multiple potential minima separated by small barrier heights.

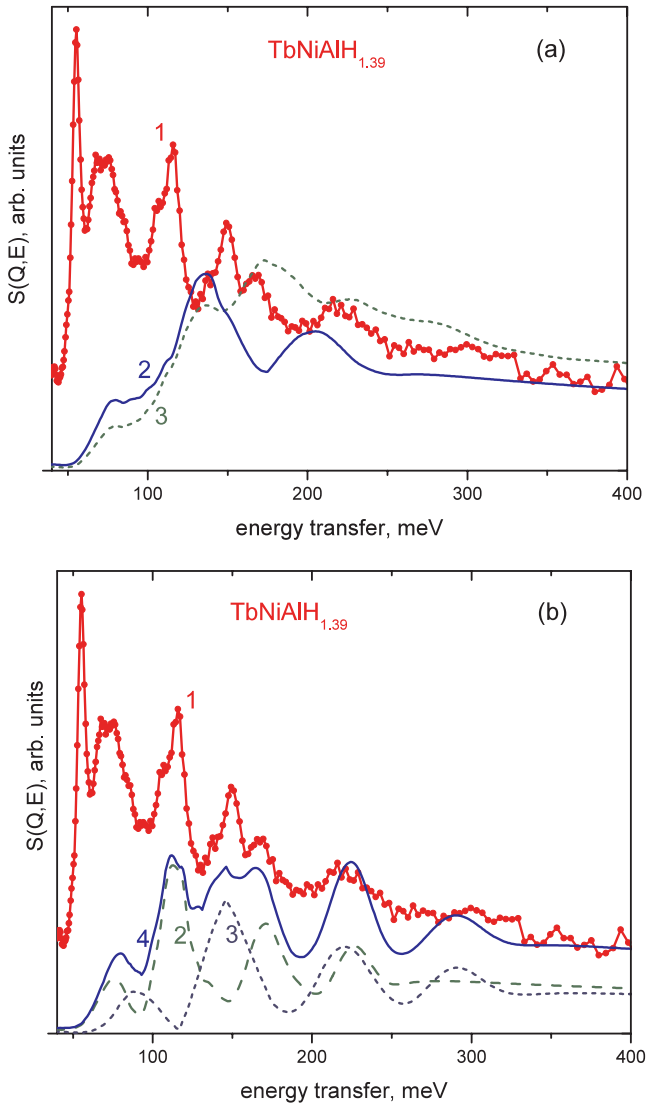

Figure 4. Calculated MPNS contributions to the INS spectrum for $TbNiAlH_{1.4}$. The curves with points show the experimental data: (a) corresponds to MPNS considering one phonon band between 43–90 meV (solid curve) and for one phonon band between 43–130 meV (dashed curve); (b) the dashed curve corresponds to MPNS obtained assuming that the one-phonon part is around the peak at 55 meV; the dotted curve assumes a one-phonon peak around 72 meV, while the solid curve is their sum. This is consistent with the structural results obtained by NPD, where two different (non-equivalent) hydrogen atoms have observed.

Acknowledgments

This work has benefited from the use of facilities at the Manuel Lujan Jr Neutron Science Center and the Advanced Photon Source. It was financially supported by the Department of Energy, Basic Energy Sciences (contracts W-7405-ENG-36 and W-31-109-ENG-38). AVK acknowledges support from the Grant Agency of the Czech Republic (202/01/P092) and HN support from NSF (DMR–0094241).

Appendix. Multiphonon neutron scattering calculation

The dynamical structure factor [25] for hydrogen-containing materials can be written as the sum of INS contributions $S_{l,k-l}(Q, E)$, due to annihilation of l and creation of $k-l$ excitations,

$$S(Q,E) = \sum_{l,k} S_{l,k-l}(Q,E) = \sum_{l,k} \frac{\sigma_{\mathrm{H}}^{inc}}{4\pi} \exp(-2W(Q)) \times \left(\frac{\hbar^2 Q^2}{6m}\right)^k \int \mathrm{d}\omega_1 \cdots \mathrm{d}\omega_k \, \frac{G(\omega_1)\cdots G(\omega_k)}{\omega_1 \cdots \omega_k (k-l)!\,l!} \times \prod_{i=l+1}^{k} [n_B(\omega_i)+1] \prod_{j=1}^{l} n_B(\omega_j)\, \delta\left(E - \sum_{i=l+1,k} \hbar\omega_i + \sum_{j=1,l} \hbar\omega_j\right). \tag{A.1}$$

Here $n_B(\omega)$ is the population Bose factor, m is the neutron mass, and $W(Q)$ is a Debye–Waller factor for a hydrogen atom. The $G(\omega)$ function is a generalized vibrational density of states for a hydrogen atom, weighted by the squared amplitudes of the atomic oscillations.

This equation can be applied to estimate the MPNS contributions by using the measured data and an iterative technique (see e.g. [26]). As the first iterative step, $G(\omega)$ and $W(Q)$ can be calculated from the experimental data based on the assumption that the experimental INS spectrum in the estimated one-phonon range is the one-phonon spectrum. In the second and subsequent steps, the difference between the experimental spectrum and that resulting from the multiphonon processes is taken as the new one-phonon spectrum. For most of the INS spectra, convergence can usually be reached in several (3–4) iterations.

The multiphonon calculations become rather time-consuming if the number of phonons involved is larger than 4 ($n \geqslant 5$). Therefore, calculations for higher n can be made using the Sjölander approximation [27]. This approximation is based on the result that convoluting a function of an arbitrary form n times, one obtains for large n a Gaussian distribution (central limit theorem of probability theory) with a mean energy value E and variance Δ which are n times greater than the mean value and variance of the energy for the initial function.

The cross-section for MPNS in the Sjölander approximation can be written in the form

$$\sigma_{Sjol} = \frac{k}{k_0} \frac{\sigma_{\mathrm{H}}^{inc}}{4\pi} F_{\mathrm{H}} \exp(E_{\mathrm{H}}\omega/\Delta_{\mathrm{H}}^2) \frac{1}{\Delta_{\mathrm{H}}} \Phi(z_{\mathrm{H}}, x_{\mathrm{H}}) \tag{A.2}$$

where

$$\Phi(z_{\mathrm{H}}, x_{\mathrm{H}}) = \sum_{n=n_0}^{m} [z_{\mathrm{H}}^n/(2\pi n)^{1/2} n!] \exp(-x_{\mathrm{H}}^2/2n), \tag{A.3}$$

$$z_{\mathrm{H}} = \frac{1}{3} \exp(-E_{\mathrm{H}}^2/2\Delta_{\mathrm{H}}^2) \int_0^\infty \frac{\hbar Q^2}{2M_{\mathrm{H}}\omega} G(\omega)[2n_B(\omega)+1]\,\mathrm{d}\omega, \tag{A.4}$$

$$x_{\mathrm{H}} = \omega/\Delta_{\mathrm{H}}, \tag{A.5}$$

$$E_{\mathrm{H}} = (\langle\hbar\omega\rangle)_{\mathrm{H}} = \int_0^\infty G(\omega)\,\mathrm{d}\omega \Big/ \int_0^\infty \frac{G(\omega)}{\omega}[2n_B(\omega)+1]\,\mathrm{d}\omega, \tag{A.6}$$

$$\Delta_{\mathrm{H}}^2 = [\langle(\hbar\omega)^2\rangle]_{\mathrm{H}} - E_{\mathrm{H}}^2 = \int_0^\infty G(\omega)\omega[2n_B(\omega)+1]\,\mathrm{d}\omega \Big/ \int_0^\infty \frac{G(\omega)}{\omega}[2n_B(\omega)+1]\,\mathrm{d}\omega - E_{\mathrm{H}}^2. \tag{A.7}$$

For many crystals the mean value and variance of the energy are comparable values, $\Delta_{\mathrm{H}} \sim E_{\mathrm{H}}$, and as a result the multiphonon cross-section calculated in the Sjölander approximation is a rather smooth function of energy. Therefore, the use of this approximation turns out to be most appropriate for cases where processes are described starting with a sufficiently large phonon content ($n > 4$). For small n_0, its use leads to incorrect results.

References

[1] Javorsky P, Burlet P, Ressouche E, Sechovsky V, Michor H and Lapertot G 1996 *Physica* B **225** 230
[2] Javorsky P, Burlet P, Sechovsky V, Andreev A V, Brown J and Svoboda P 1997 *J. Magn. Magn. Mater.* **166** 133
[3] Brück E, Nakotte H, de Boer F R, de Châtel P F, van der Meulen H P, Franse J J M, Menovsky A A, Kim Ngan N H, Havela L, Sechovsky V, Perenboom J A A J, Tuan N C and Sebek J 1994 *Phys. Rev.* B **49** 8852
[4] Sechovsky V and Havela L 1998 Magnetism of ternary intermetallic compounds of uranium *Handbook of Magnetic Materials* vol 11, ed K H J Buschow (Amsterdam: Elsevier)
[5] Kolomiets A V, Havela L, Yartys V A and Andreev A 1997 *J. Alloys Compounds* **253/254** 343
[6] Zogal O J, Lam D J, Zygmunt A, Drulis H, Petrynski W and Stalinski S 1984 *Phys. Rev.* B **29** 4837
[7] Kolomiets A V, Havela L, Rafaja D, Bordallo H N, Nakotte H, Yartys V A, Hauback B C, Drulis H, Iwasieczko W and DeLong L E 2000 *J. Appl. Phys.* **87** 6815
[8] Brinks H W, Yartys V A, Hauback B C and Fjellvag H 2002 *J. Alloys Compounds* **330–332** 169
[9] Raj P, Shashikala K and Sathyamoorthy A 2001 *Phys. Rev.* B **63** 94414
[10] Sears V F 1992 *Neutron News* **3** 29
[11] Bordallo H N, Nakotte H, Kolomiets A V, Christianson A, Havela L, Shultz A J, Drulis H and Iwasieczko W 2000 *Physica* B **276–278** 706
[12] Yamamoto T, Ishi Y and Kayano H 1998 *J. Alloys Compounds* **269** 162
[13] Raj P, Shashikala K, Sathyamoorthy A, Malik S K and Yelon W B 2001 *J. Appl. Phys.* **89** 11
[14] Sivia D S, Vorderwisch P and Silver R N 1990 *Nucl. Instrum. Methods Phys. Res.* A **290** 492
[15] Yartys V A, Gingl F, Yvon K, Akselrud L G, Kolomiets A V, Havela L, Vogt T, Harris I R and Hauback B C 1998 *J. Alloys Compounds* **279** L4
[16] Hauback B C, Fjellvag H, Palhaugen L, Yartys V A and Yvon K 1999 *J. Alloys Compounds* **293–295** 178
[17] Bordallo H N, Nakotte H, Eckert J, Kolomiets A V, Havela L, Andreev A V, Drulis H and Iwasieczko W 1998 *J. Appl. Phys.* **83** 6986
[18] Larson A C and Von Dreele R B 1986 *Los Alamos National Laboratory Report* L-UR-86-748
[19] Bashkin I O, Kolesnikov A I and Ponyatovsky E G 1995 *High Pressure Res.* **14** 91
[20] Agranovich V M and Lalov I I 1987 *Spectroscopy and Excitation Dynamics of Condensed Molecular Systems* ed V M Agranovich and R M Hochstrasser (Moscow: Nauka) p 427
[21] Agranovich V M, Dubovskii O A and Orlov A V 1986 *Phys. Lett.* A **119** 83
[22] Agranovich V M and Dubovskii O A 1986 *Int. Rev. Phys. Chem.* **5** 93
[23] Agranovich V M, Dubovskii O A and Orlov A V 1989 *Solid State Commun.* **70** 675
[24] Ross D K, Antonov V E, Bokhenkov E L, Kolesnikov A I, Ponyatovsky E G and Tomkinson J 1998 *Phys. Rev.* B **58** 2591
[25] Marshall W and Lovesey S W 1971 *Theory of Thermal Neutron Scattering* (Oxford: Clarendon)
[26] Antonov V E, Belash I T, Kolesnikov A I, Mayer J, Natcaniec I, Ponyatovskii E G and Fedotov V K 1991 *Sov. Phys.–Solid State* **33** 87
[27] Sjölander A 1958 *Ark. Fys.* **14** 316